Received: 23 February 2016 | Revised: 2 December 2016 | Accepted: 15 December 2016

DOI 10.1111/cmi.12713

WILEY

RESEARCH ARTICLE

Soluble *N*-ethylmaleimide-sensitive factor attachment protein receptors required during *Trypanosoma cruzi* parasitophorous vacuole development

Juan Agustín Cueto[1,2] | María Cristina Vanrell[1] | Betiana Nebaí Salassa[1] | Sébastien Nola[3] | Thierry Galli[3] | María Isabel Colombo[1] | Patricia Silvia Romano[1]

[1] Laboratorio de Biología de Trypanosoma cruzi y la célula hospedadora - Instituto de Histología y Embriología (IHEM) "Dr. Mario H. Burgos" CCT CONICET Mendoza, Facultad de Ciencias Médicas, Universidad Nacional de Cuyo-CONICET, Mendoza, Argentina

[2] Instituto de Fisiología, Facultad de Ciencias Médicas, Universidad Nacional de Cuyo, Mendoza, Argentina

[3] Membrane Traffic in Health & Disease, INSERM ERL U950, Univ Paris Diderot, Sorbonne Paris Cité, Institut Jacques Monod, Paris, France

Correspondence
Patricia S. Romano, Laboratorio de Biología de *Trypanosoma cruzi* y la célula hospedadora, Instituto de Histología y Embriología "Dr. Mario H. Burgos", CCT CONICET Mendoza. Facultad de Ciencias Médicas UNCuyo – CONICET. Casilla de correo 56, Mendoza, Argentina CP 5500.
Email: promano@fcm.uncu.edu.ar

Abstract

Trypanosoma cruzi, the etiologic agent of Chagas disease, is an obligate intracellular parasite that exploits different host vesicular pathways to invade the target cells. Vesicular and target soluble *N*-ethylmaleimide-sensitive factor attachment protein receptors (SNAREs) are key proteins of the intracellular membrane fusion machinery. During the early times of *T. cruzi* infection, several vesicles are attracted to the parasite contact sites in the plasma membrane. Fusion of these vesicles promotes the formation of the parasitic vacuole and parasite entry. In this work, we study the requirement and the nature of SNAREs involved in the fusion events that take place during *T. cruzi* infection. Our results show that inhibition of *N*-ethylmaleimide-sensitive factor protein, a protein required for SNARE complex disassembly, impairs *T. cruzi* infection. Both TI-VAMP/VAMP7 and cellubrevin/VAMP3, two v-SNAREs of the endocytic and exocytic pathways, are specifically recruited to the parasitophorous vacuole membrane in a synchronized manner but, although VAMP3 is acquired earlier than VAMP7, impairment of VAMP3 by tetanus neurotoxin fails to reduce *T. cruzi* infection. In contrast, reduction of VAMP7 activity by expression of VAMP7's longin domain, depletion by small interfering RNA or knockout, significantly decreases *T. cruzi* infection susceptibility as a result of a minor acquisition of lysosomal components to the parasitic vacuole. In addition, overexpression of the VAMP7 partner Vti1b increases the infection, whereas expression of a KIF5 kinesin mutant reduces VAMP7 recruitment to vacuole and, concomitantly, *T. cruzi* infection. Altogether, these data support a key role of TI-VAMP/VAMP7 in the fusion events that culminate in the *T. cruzi* parasitophorous vacuole development.

1 | INTRODUCTION

Trypanosoma cruzi is the causative agent of Chagas disease. Chagasic cardiomyopathy and digestive tract abnormalities are clinical manifestations of the chronic phase and the responsible for high mortality. This parasitic disease is found in endemic areas of Latin America, but different factors have determined its occurrence in other latitudes (Rassi & Marin-Neto, 2010; Hotez et al., 2012).

T. cruzi is an obligate intracellular pathogen that infects a wide variety of cells, including professional and nonprofessional phagocytic cells. It is well established that *T. cruzi* resides transiently in a membrane bound vacuole called parasitophorous vacuole. Acquisition of lysosomal markers (e.g., LAMP1 and LAMP2) by the *T. cruzi* parasitophorous vacuole (TcPV) is essential to retain the parasite intracellularly and establish a productive infection (Andrade & Andrews, 2004; Albertti, Macedo, Chiari, Andrews, & Andrade, 2010). The subsequent acidification of the TcPV allows the parasite to disrupt the vacuolar membrane and gains access to the host cytoplasm, where it differentiates into amastigotes (Ama) and begins intracellular replication (Ley, Robbins, Nussenzweig, & Andrews, 1990; Andrade & Andrews, 2004).

Studies of the mechanism that allows trypomastigotes (Try), the infective stage of *T. cruzi*, reaching host cell lysosomes in nonprofessional phagocytic cells have disclosed different strategies (Romano et al., 2012). The first involves lysosomes exocytosis at the site of parasite attachment (Tardieux et al., 1992), suggesting that lysosomes provide the membrane required for TcPV formation. Further studies established that this mechanism is intimately related with the mechanism of host cell plasma membrane repair triggered by mechanical wounding caused by *T. cruzi* (Fernandes et al., 2011; Fernandes,

Corrotte, Miguel, Tam, & Andrews, 2015). Exploiting this pathway, Try bypass other cellular pathways to directly target lysosomes. Although, this mechanism is deeply rooted in the scientific community, alternative routes for *T. cruzi* entry were further proposed. Long afterward, Woolsey et al. (2003) disclosed a second mechanism that involves the formation of a plasma membrane-derived vacuole enriched in PtdIns*P*3 and PtdIns(3,4)*P*2, lipid products of class I PI 3-kinases. Also, a subsequent interaction of this vacuole with key proteins of the endocytic trafficking machinery (i.e., dynamin, EEA1, Rab5, and Rab7) before lysosomal interaction occurs was reported (Wilkowsky, Barbieri, Stahl, & Isola, 2002; Woolsey et al., 2003; Barrias, Reignault, Souza, & Carvalho, 2010; Caradonna & Burleigh, 2011). Subsequently, our laboratory found the interaction between Try and the host cell autophagic pathway during infection, based on the presence of the autophagosomal marker LC3 at parasite entry sites and PV (Romano, Arboit, Vázquez, & Colombo, 2009). Recently, Barrias, Reignault, Souza, and Carvalho (2012) further demonstrated that Try can invade the cell through macropinocytosis. All these data support the idea that *T. cruzi* exploits several available mechanisms to enter host cells.

Regardless of parasite entry strategy, successful colonization of host cell requires membrane fusion events. Soluble NSF (*N*-ethylmaleimide-sensitive fusion protein) attachment receptors (SNAREs) constitute the core machinery of intracellular membrane fusion, the final stage of every intracellular vesicle transport pathway in eukaryotes. For us to accomplish this, a vesicular SNARE (v-SNARE) and its partners located on target membranes (t-SNAREs) interact to form a so-called trans-SNARE complex to drive membrane fusion. Afterwards, NSF and αSNAP (Soluble *N*-ethylmaleimide-sensitive factor attachment protein) bind to the resulting cis-SNARE complex. NSF, which has both Adenosine triphosphate (ATP) binding and hydrolyzing activity, is a key protein required for SNARE-mediated vesicular fusion (Zhao, Smith, & Whiteheart, 2012). Indeed, once fusion process has occurred, complementary SNAREs remain paired in a fusogenically inactive configuration (i.e., cis-SNARE complex). Subsequent NSF ATPase activity is required to allow dissociation of the cis-SNARE complex rendering free SNAREs available for the next round of fusion (Moeller et al., 2012).

The current understanding of SNARE action also points that different SNAREs localize specifically on the different intracellular membrane compartments. Only appropriate combinations of v-SNARE and t-SNARE lead to membrane fusion. Among the nine v-SNAREs identified in mammals, VAMP3 and VAMP7 stick out for their involvement in endosomal membrane fusion. VAMP3 located on early and recycling endosomes and VAMP7 on late endosomes and post-Golgi secretory vesicle. VAMP3 is proteolysed by tetanus neurotoxin (TeNT), like its neuronal counterparts VAMP1 and VAMP2, whereas VAMP7 is resistant to TeNT (Proux-Gillardeaux, Rudge, & Galli, 2005) and has a regulatory amino-terminal extension called longin domain (Daste, Galli, & Tareste, 2015). VAMP3 regulates endosomal receptor recycling (Galli et al., 1994; Breton et al., 2000). Most recently, VAMP3 has been implicated in the fusion of multivesicular bodies with autophagosomes generating a hybrid organelle termed amphisome (Fader, Sánchez, Mestre, & Colombo, 2009). VAMP7 has been involved in trafficking from late endosomes to lysosomes (Advani, 1999) and fusion between autophagosomes and lysosomes (Fader et al., 2009). There is also evidence that links VAMP7 to the exocytosis of diverse cargos from lysosomes (Rao, Huynh, Proux-Gillardeaux, Galli, & Andrews, 2004; Verderio et al., 2012) and autophagosomes (Fader, Aguilera, & Colombo, 2012). Finally, endobrevin/VAMP8 (hereafter referred to as VAMP8) has been involved in the homotypic fusion between late endosomes (Advani, 1999) and also in regulated exocytosis (Wang et al., 2007).

In summary, in this study we sought to identify components of the membrane fusion machinery involved in the interaction between the host cell endocytic compartments and TcPV. We find that TI-VAMP/VAMP7 plays a major role in the maturation of the TcPV in non-phagocytic cells.

2 | RESULTS

2.1 | *T. cruzi* entry is an NSF-dependent process

To assess the importance of NSF on parasite–host cell entry, we treated cells with *N*-ethylmaleimide (NEM), a largely known inhibitor of NSF activity (Woodman, 1997). For this purpose, chinese hamster ovary (CHO) cells were incubated with 50 μM of NEM, for 10 min, then washed, and subjected to infection for 3 hr. Quantification showed a significant decrease in the percentage of infection, ranging from 36 ± 3.0% in control cells to 16.8 ± 0.2% when NSF activity was pharmacologically inhibited (Figure 1a).

For us to confirm this observation, CHO cells were transiently transfected with GFP-tagged plasmids encoding wild-type NSF (WT NSF) or the dominant-negative ATPase-deficient mutant (NSF D1EQ; Nagiec & Whiteheart, 1995), and then cells were infected with *T. cruzi* for 3 hr. As expected, overexpression of the NSF mutant displayed a significant decrease in the percentage of infected cells compared to vector transfected and non-transfected cells. In contrast, WT NSF resulted in a remarkably increase of this value (Figure 1b).

Taking together, these results show that *T. cruzi* entry can be modulated by NSF activity confirming the participation of SNARE proteins on this process.

2.2 | v-SNAREs from the endocytic pathway are recruited to the *T. cruzi* parasitophorous vacuole

According to the SNARE model, it is expected that SNAREs involved in TcPV formation would be displayed on its limiting membrane as a result of fusion events (Bombardier & Munson, 2015). For this reason, we investigated the presence of three different v-SNAREs based on their role in trafficking pathways previously related with *T. cruzi* host cell entry (Romano et al., 2012).

For us to determine the association of these SNARE proteins, CHO cells were transiently transfected with GFP-tagged plasmids encoding for the selected VAMPs and then infected for 3 hr. As shown in Figure 2a and 2b, a large percentage of the TcPV population was decorated with GFP-VAMP7 (68.7% ± 12.2%), whereas GFP-VAMP3 was only detected in a minor fraction of vacuoles (30.2% ± 15.0%). In contrast, GFP-VAMP8 was not found to significantly accumulate around the vacuole. As shown in Figure 2a, GFP-VAMP7 was distributed in a patchy pattern around the TcPV. Endogenous VAMP7 was

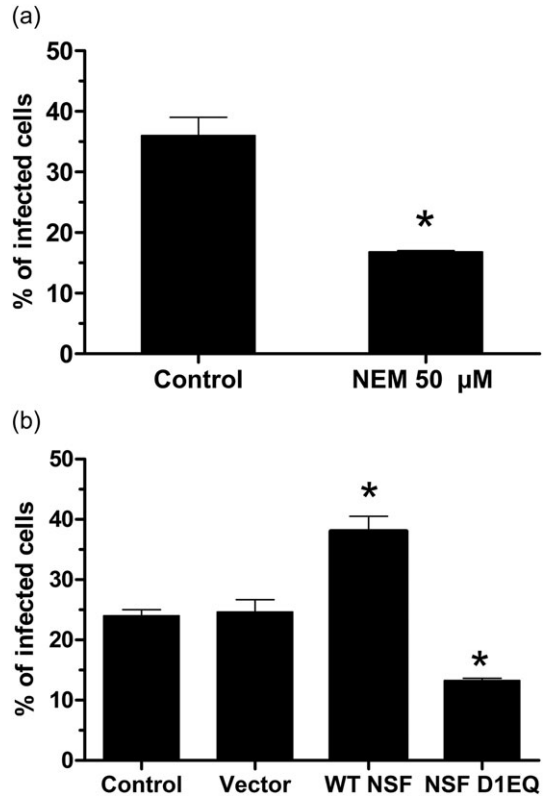

FIGURE 1 Role of host *N*-ethylmaleimide (NEM)-sensitive factor (NSF) in the *Trypanosoma cruzi* trypomastigotes invasion process. (a) Chinese hamster ovary (CHO) cells were treated with NEM (50 μM; 10 min at room temperature) or not (control) and then infected with *T. cruzi* trypomastigotes for 3 hr. Afterward, cells were fixed and processed for immunofluorescence detection of parasites. Infection rate were quantified by confocal microscopy and expressed as percentage of infected cells. The bar graph shows a marked inhibition of cellular infection when treated with NEM compared to control. (b) CHO cells were transiently transfected with either EGFP vector alone, EGFP-NSF, or EGFP-NSF D1EQ and then infected and processed as described in (a). Non-transfected CHO cells (control) were used to test the effect of the transfection itself over the cellular susceptibility to infection. The bar graph shows an increased infection rate in EGFP-NSF-expressing cells and a diminished infection rate in EGFP-NSF D1EQ-expressing cells when compared with vector transfected cells. (a and b) The data correspond to the mean of three independent experiments ±SEM. $^*p < .05$, Student's *t* test

also detected in close proximity with TcPV, in good agreement with the distribution pattern of the overexpressed GFP-tagged protein (Figure 2c).

To gain insights into the dynamics of VAMP7 acquisition by TcPV, we performed time-lapse video microscopy. GFP-VAMP7 transfected CHO cells were infected with *T. cruzi* for 1 hr and placed into a thermostatic chamber. Parasites were labeled by means of a mitochondrial vital stain (MitoTracker® Red, Molecular Probes). Figure 3 (micrographs extracted from movie S1) shows the membrane of a TcPV enriched with VAMP7 and some tiny VAMP7 vesicles scattered throughout the host cell cytoplasm (0 min). A VAMP7 vesicle can be seen progressively approaching the TcPV (1–3 min) to finally merge with it (4–5 min), indicating that VAMP7-positive vesicles effectively fuse with the TcPV. Altogether, these results suggest that VAMP7 vesicles are in close proximity and fuse with TcPV.

2.3 | VAMP7 and VAMP3 are recruited to the TcPV at different times during infection

The above results prompted us to analyze the kinetics of recruitment of both VAMP7 and VAMP3. Due to LAMP1 has been extensively used for tracking the parasite intracellular fate, we decided to also analyze its recruitment to TcPV. For us to do this, CHO cells overexpressing GFP-VAMP7, GFP-VAMP3, or mCherry-LAMP1 were infected for 15 min. After this time, extracellular parasites were removed by washing, and one coverslip of each condition, corresponding to the first time point (15 min), was immediately fixed. The other samples were incubated for an additional period to complete a total assay time of 1, 3, 6, and 12 hr before fixation.

As early as 15-min post-infection (p.i.), we found VAMP7 associated in a patchy pattern to a partially internalized parasite (Figure 4a). As cell invasion progressed, VAMP7 was enriched around parasites to finally surround them completely (6-hr p.i.). As expected, at later infection times (i.e., 12-hr p.i.), VAMP7 completely dissipated from the internalized parasites. On the other hand, interaction of VAMP3 with internalized parasites was observed at early times (Figure 4a, 15 min and 1 hr). However, this association was no longer observed when infected host cells were incubated for prolonged periods. It is interesting to note the morphological transition underwent by the parasite throughout the course of the invasion process, from the typical elongated form of Try at early times (up to 3 hr) to the ovoid form of Ama at later times (6 hr onwards).

Quantification of this assay (Figure 4b) revealed a modest percentage of intracellular parasites associated with VAMP7 at 15-min p.i. (27.2 ± 5.8%). However, the main peak occurred at 3-hr p.i. (82.3 ± 11.4%) and declined thereafter to reach almost 0 at 12 hr. The TcPV acquisition of VAMP3 was different, because 72.5 ± 0.5% of the TcPVs were already positive for VAMP3 at 15 min. VAMP3 recruitment was still high at 1-hr p.i. (69.6 ± 1.8%), decaying abruptly afterwards. As expected, the timing of LAMP1 acquisition mainly paralleled that observed for VAMP7. This low recruitment of LAMP1 at the site of Try entry should be reinterpreted in the light of results published by Cortez, Real, and Yoshida (2015). They proved that metacyclic Try generated in vitro (equivalent of insect-borne parasite form) need lysosomal exocytosis to get inside cells, whereas tissue culture-derived Try (equivalent of bloodstream parasite form), the same parasite form used in this work, did not require lysosomes for invasion, although later they resulted absolutely necessary to establish an effective internalization.

Additionally, we compared the kinetics of VAMP7 and VAMP3 association with phagosomes formed following fibronectin-coated 3 μm latex beads uptake. We found that the kinetics of VAMP7 and VAMP3 acquisition during phagosome maturation were similar to those observed for TcPV (Fig. S1A), although VAMP7 recruitment to phagosome remained high even up to 12 hr. This distinguishing feature is determined by the parasite-driven disruption of its vacuole. To rule out any possibility of VAMP7 acquisition to the TcPV through phagocytosis (Braun et al., 2004), we took advantage of the property of latrunculin B to depolymerize actin filaments that eventually leads to phagocytosis inhibition. To accomplish this, we first transfected CHO cells with GFP-VAMP7 and treated with latrunculin B (0.1 μM) or

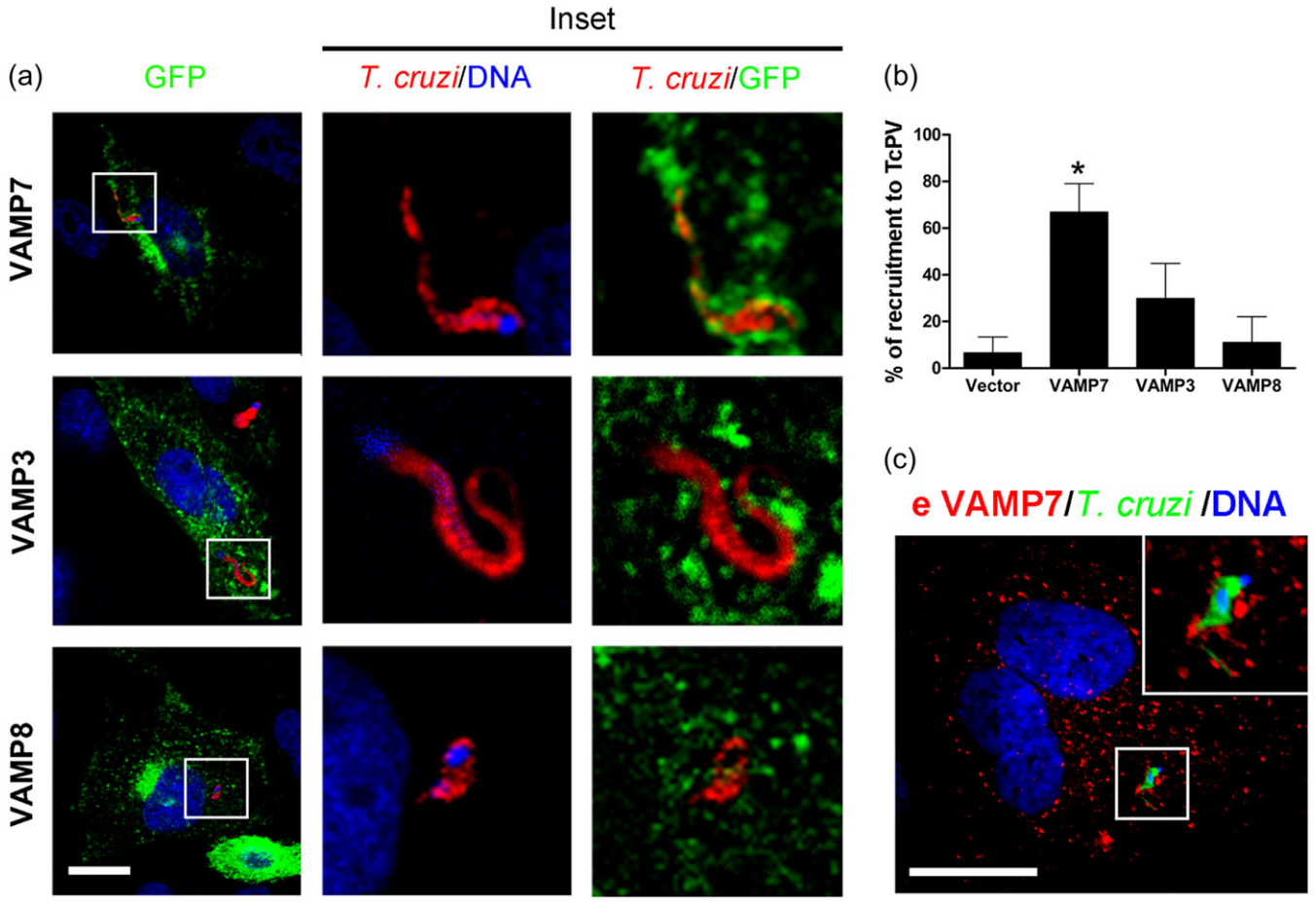

FIGURE 2 Association of *Trypanosoma cruzi* parasitophorous vacuoles with host cell endocytic SNAREs. Chinese hamster ovary cells transiently expressing EGFP-VAMP7, EGFP-VAMP3, and EGFP-VAMP8 were infected with *T. cruzi* trypomastigotes for 3 hr. Cells were then fixed, subjected to indirect immunofluorescence to detect *T. cruzi*, and stained with Hoechst 33258 to visualize cell and parasite nuclei, as well as parasite kinetoplast DNA. The number of TcPVs associated with SNAREs was determined by confocal microscopy. (a) The confocal image shows a dense punctate pattern of VAMP7 outlining an intracellular parasites (upper panels). In the case of VAMP3, a sparse punctate pattern can be seen around *T. cruzi* vacuole, although the recruitment is most notorious on the kinetoplast region (middle panels). However, VAMP8 does not show a clear association with TcPV (lower panels). Insets show higher magnification of framed regions. (b) The bar graph shows high proportion of TcPVs associated with VAMP7, a minor but still noticeable association with VAMP3 and a null association with VAMP8. The data are represented as mean ± SEM of four independent experiments. $^*p < .05$, Student's *t* test. (c) Chinese hamster ovary cells were infected with trypomastigotes for 3 hr, followed by immunofluorescent staining of parasites and endogenous VAMP7. Host cell and parasite DNA were stained with Hoechst 33258. The confocal image shows endogenous VAMP7 decorating a TcPV. Scale bar: 10 μm

DMSO for 20 min. Then, parasites or beads were added directly into the medium and incubated for 3 hr. As expected, inhibition of phagocytosis by latrunculin B treatment abolished latex beads uptake (Fig. S1B) but did not altered the rate of *T. cruzi* infected cells (Fig. S1C) and more importantly did not affect VAMP7 recruitment to the TcPV (S1D and E).

The kinetic studies indicated the presence of both VAMP3 and VAMP7 on TcPV membrane at early times after infection. To find out whether these two proteins are mutually excluded from the TcPV, we next co-transfected cells with plasmids that expressed GFP-tagged VAMP3 and RFP-tagged VAMP7. Cells were subsequently infected for 15 min or 1 hr. Interestingly, our results showed that both proteins coexist in the TcPV at earlier times after infection. VAMP3 distributed uniformly around the parasites at 15-min p.i. with little detection of VAMP7. However, both proteins could be detected in the same vacuole at 1-h p.i. (Fig. S2A). Similar to single transfected cells, the percentage of VAMP3 recruitment was high (~70%) at these time points after infection, whereas acquisition of VAMP7 increased at longer times, raising to approximately 80–90% at 1-hr p.i. (Fig. S2B). Also, we co-transfected cells with GFP-VAMP7 and mCherry-LAMP1, and we found that both proteins coexist in all the vacuoles observed at 1-h p.i. (Fig. S3). Altogether, these data suggest that VAMP3 and VAMP7 are consecutively recruited at TcPV with a period of overlap.

2.4 | VAMP7 but not VAMP3 fusion activity is required for efficient *T. cruzi* host cell infection

On the basis of our evidence that VAMP3 and VAMP7 are recruited to the TcPV, we further evaluated whether fusion of both compartments, corresponding respectively to early and late endosomes, were required for *T. cruzi* infection. For this purpose, we first took advantage of the fact that the longin domain of VAMP7 (LD) has an inhibitory effect on VAMP7-mediated fusion events (Martinez-Arca et al., 2003; Proux-Gillardeaux, Raposo, Irinopoulou, & Galli, 2007; Daste et al.,

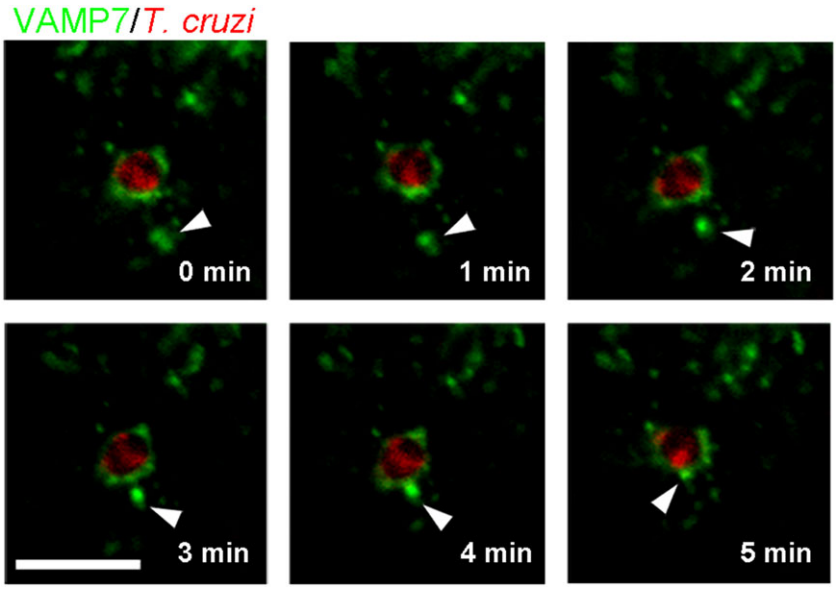

FIGURE 3 Dynamic of VAMP7 vesicles recruitment to the *Trypanosoma cruzi* parasitophorous vacuole. Chinese hamster ovary cells transiently expressing EGFP-VAMP7 WT were infected with *T. cruzi* trypomastigotes previously labeled with Mito Tracker. After 2 hr, the cells were mounted into an in vivo camera and analyzed by confocal microscopy. Selected frames from time-lapse videomicroscopy showing a VAMP7 vesicle heading to fusion with the TcPV (white arrowhead). Acquisition times are indicated in the lower left corner. Scale bar: 5 μm

2015) likely because it binds the SNARE domain of the protein (Schäfer et al., 2012). Taking into account that our plasmids contain human sequences, we decided to study the effect of the LD in HeLa cells, a human-derived cell line. These cells also recruited VAMP7 around TcPV at 3 hr as CHO cells did (Fig. S4). Thus, HeLa cells overexpressing either GFP-VAMP7 LD or GFP vector alone were infected with Try for 3 hr and processed for confocal microscopy. As depicted in Figure 5a, infection was evidently hampered in HeLa cells overexpressing VAMP7 LD, indicating that VAMP7 has a critical role in Try infection.

We then performed a siRNA knockdown assay to deplete endogenous VAMP7. Because commercial siRNA was targeted to the sequence of human VAMP7, HeLa cells were used again in this experiment. In order to verify the knockdown efficiency, we conducted a Western blot analysis was conducted to assess silencing efficiency on VAMP7 expression (Figure 5b). Cells were co-transfected either with scrambled siRNA and GFP vector or with siRNA against VAMP7 and GFP vector followed by Try infection for 3 hr. We observed that cells transfected with scrambled siRNA-displayed VAMP7 vesicles widely distributed throughout the cytoplasm and also within the Golgi area (Figure 5c, upper panels). As expected, intracellular parasites were surrounded by VAMP7 (Figure 5c, upper panel, inset). It is important to note that VAMP7-depleted cells showed no detectable VAMP7 labeling (Figure 5c, lower panels). This was accompanied by a reduction in the percentage of infected cells by nearly half when compared to the scrambled siRNA (from 46 to 24.5%; Figure 5d).

To definitely prove that *T. cruzi* infection depends on the VAMP7 fusogenic activity, we used VAMP7 knockout mouse embryonic fibroblasts (VAMP7 KO MEF) that were immortalized (see Materials and Methods). Both WT MEF and VAMP7 KO MEF were infected for 3 hr with Try and then subjected to IF to detect intracellular parasites. As expected, parasite infection was reduced from 56.8 ± 1.8% in WT MEF cells to 27.8 ± 1.1% in VAMP7 KO MEF cells (Figure 5e), thus confirming our previous results.

Functional relevance of VAMP3 on infectivity was also investigated. To this end, we took advantage of TeNT, a protease with specific activity against VAMP1, VAMP2, and VAMP3 (Humeau, Doussau, Grant, & Poulain, 2000), which targets VAMP3 in non-neuronal cells (Galli et al., 1994). For this purpose, CHO cells were transfected with GFP-VAMP3, GFP vector alone, or co-transfected with a plasmid encoding for the TeNTpCMV5 together with either GFP-VAMP3 or GFP vector. Cells were then infected with Try for 15 min or 3 hr and processed for confocal microscopy. The overexpression of TeNT altered the pattern of GFP-VAMP3 distribution from punctate structures to a diffuse distribution, which indicates that VAMP3 was efficiently cleaved (data not shown). However, to our surprise, neither VAMP3 nor TeNT overexpression affected the percentage of infected cells at the two times tested when compared with GFP vector in the studied cell lines (Fig. S5). We also performed the same assay with HeLa for just 3 hr of infection with similar result (Fig. S5). Altogether, our results suggest that VAMP7 plays an essential role in *T. cruzi* host cell infection, whereas VAMP3 is dispensable.

2.5 | Interaction between TcPV and lysosomes is impaired by the loss of VAMP7

The previous results suggest that late endosome and lysosome fusion mediated by VAMP7 plays a critical role in *T. cruzi* host cell infection, likely because lysosome fusion with TcPV may be a critical event in this process. In this regard, the occurrence of LAMP1, a late endosomal/lysosomal marker, has been widely used to assert this fusion event. Therefore, to determine if the absence of VAMP7 would impair the fusion of lysosomes with TcPV, we search for the presence of TcPVs labeled with LAMP1. VAMP7 KO MEF and WT MEF cells were infected for 3 hr with Try and then subjected to a double IF to detect intracellular parasites and LAMP1. Figure 6a (upper panel) shows LAMP1 puncta outlining internalized parasites in WT MEF cells, corroborating previous reports (Caler, Chakrabarti, Fowler, Rao, & Andrews, 2001; Fernandes et al., 2011; Zhao et al., 2013; Cortez et al., 2015). However, in VAMP7 KO MEF cells, LAMP1 labeling was less evident in the TcPV membrane (Figure 6a , lower panel). Quantitative data revealed that 74.0 ± 1.6% of the internalized parasites were surrounded by LAMP1 in WT MEF cells, whereas this index dropped down to 42.3 ± 2.1% in VAMP7 KO MEF cells (Figure 6b).

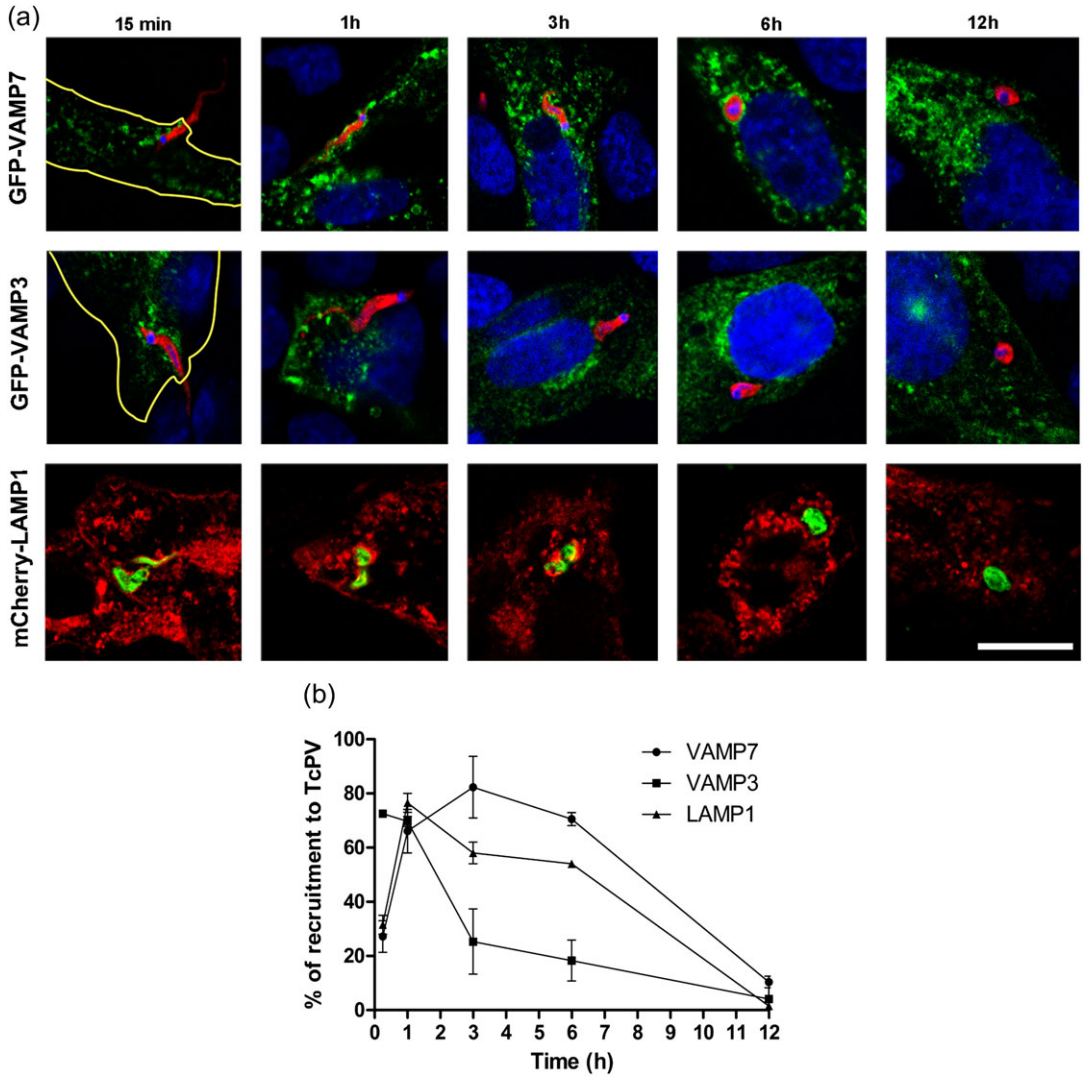

FIGURE 4 Time course of VAMP7 and VAMP3 acquisition on *Trypanosoma cruzi* parasitophorous vacuoles during infection. Chinese hamster ovary cell were transfected with EGFP-VAMP7, EGFP-VAMP3, or mCherry-LAMP1 and infected for 15 min with *T. cruzi* trypomastigotes. After this period, cells were washed extensively to remove non-internalized parasites and incubated for an additional period, resulting in a total assay time of 1, 3, 6, and 12 hr. Cells were then fixed, subjected to indirect immunofluorescence to detect *T. cruzi*, and stained with Hoechst 33258 to visualize cell and parasite nuclei. (a) Confocal images showing the time-dependent recruitment of both VAMP7 (upper panel), VAMP3 (middle panel), and LAMP1 (lower panel) to the TcPV. (b) The scatter plot analysis indicates that parasites are highly associated with VAMP3 at early time points during invasion and then decay progressively, whereas VAMP7 and LAMP1 is gradually acquired, reached a peak at 1–3-hr post-infection and decayed afterward. Scale bar: 10 μm

Additionally, we performed a time-lapse video microscopy to study the dynamic of the interaction between lysosomes and TcPV. For us to achieve this goal, VAMP7 KO MEF and WT MEF cells were incubated with LysoSensor® Green, an acidotrophic probe with a pH-dependent fluorescence and then exposed to MitoTracker red-labeled Try for 2 hr. Time-lapse imaging showed that delivery of lysosomal content into the TcPV is a common phenomenon in WT MEF cells (Movie S2). This process leads to luminal acidification of TcPV, evidenced by a sharp green fluorescent outline around the parasite and eventually some brighter areas representing lower pH (Figure 7, upper panel). However, we failed to observe lysosome-TcPV fusion events in VAMP7 KO MEF cells by time-lapse imaging, most likely because this phenomenon is less frequent in the absence of VAMP7. This could explain the fact that TcPVs are less acidic in VAMP7 KO MEF cells as indicated by the weak green LysoSensor fluorescence (Figure 7, lower panel).

2.6 | VAMP7 cognate partners and KIF5 are involved in TcPV formation

VAMP7 forms tetrameric trans-SNARE complexes with both plasma membrane and endosomal t-SNAREs. In non-neuronal cells, VAMP7 mediates lysosomes exocytosis thorough its interaction with plasma membrane-localized partners, such as Stx3, Stx4, and SNAP23 (Chaineau, Danglot, & Galli, 2009). VAMP7 also forms SNARE complexes with the endosomal t-SNAREs Stx7, Stx8, and Vti1b to allow late endosome/lysosome fusion (Pryor et al., 2004).

To disclose the relative importance of these two pathways in the invasion process, we selected arbitrarily a cognate partner representative of each group. Thus, CHO cells overexpressing either GFP-SNAP23 or GFP-Vti1b were infected with Try for 3 hr and processed for confocal microscopy. Representative images of TcPVs displaying

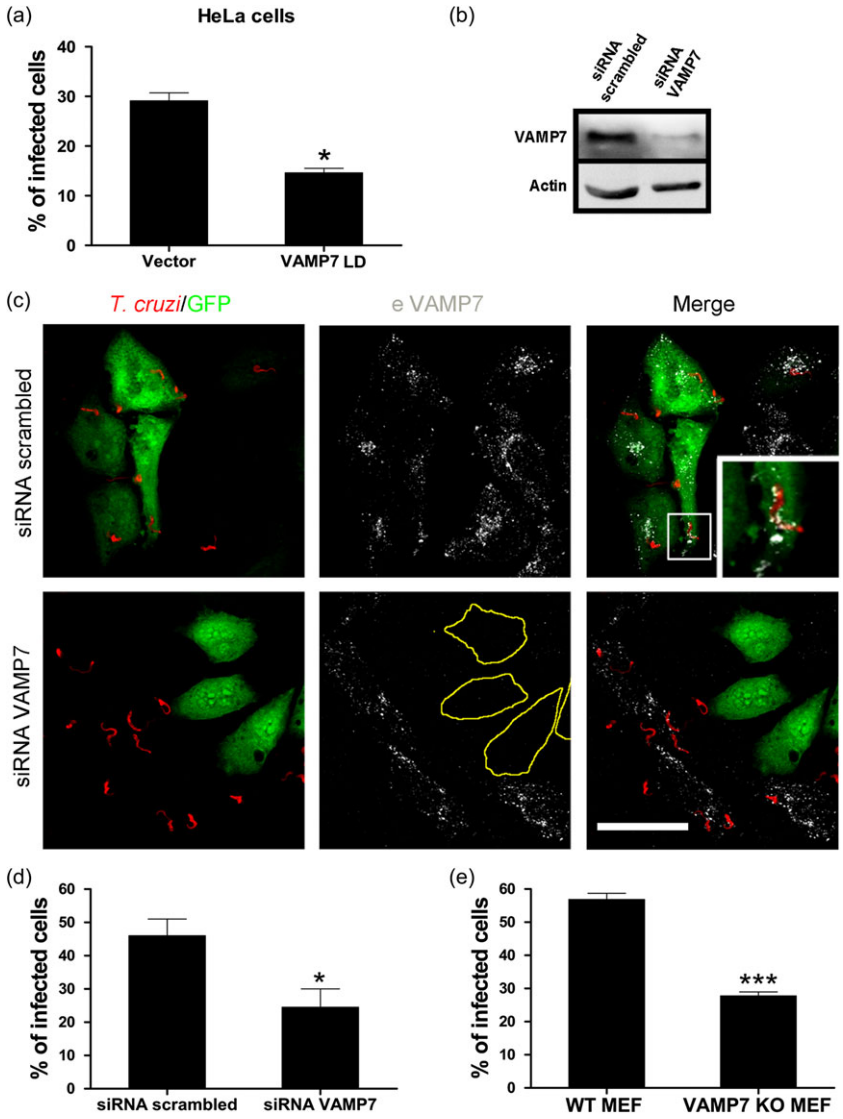

FIGURE 5 Effect of VAMP7 depletion on host cell susceptibility to infection. (a) HeLa cells were transfected with either GFP vector alone or GFP-VAMP7 LD constructs and infected with *T. cruzi* trypomastigotes for 3 hr. Subsequently, cells were fixed and subjected to indirect immunofluorescence to detect *T. cruzi*. Infection level was quantified by confocal microscopy and expressed as percentage of infected cells. (a) Overexpression of VAMP7 LD in HeLa cells effectively reduces the infection when compared with the vector. (b) Efficiency of VAMP7 silencing was verified by Western blot. (c) HeLa cells were co-transfected with EGFP vector and either scrambled siRNA or siRNA directed against VAMP7. After 48 hr of treatment, cells were infected for 3 hr and subjected to a double immunofluorescence using specific antibodies for *T. cruzi* and VAMP7. Confocal images showing that scrambled siRNA transfection does not affect VAMP7 recruitment around internalized parasites (upper panel). VAMP7 siRNA transfected cells are depleted of endogenous VAMP7 (cells delimited by yellow line; lower panel). Inset shows higher magnification of framed regions. Scale bar: 15 μm. (d) Quantitative analysis reveals that VAMP7 knockdown reduces the percentage of infected cells. (e) VAMP7 KO MEF cells and WT MEF cells were infected with Try for 3 hr and then analyzed by immunofluorescence staining to detect internalized parasites. Quantitative analysis shows that VAMP7 KO MEF cells are less infected than WT MEF cells. The data are represented as means ± SEM of three independent experiments. $^{*}p < .05$; $^{***}p < .005$, Student's *t* test

SNAP23 and Vti1b on its membrane are shown in Figure 8a. Although both proteins are present at the vacuole membrane, Vti1b recruitment was higher than SNAP23 at this time point (Figure 8b). In agreement to this data, the percentage of infected cells significantly increased in Vti1b overexpressing cells compared to control. This result indicates that, in contrast to plasma membrane partners, late endosomal/lysosomal partners are involved in fusion processes with the TcPV at 3-hr p.i.

In order to gain a better understanding of the molecular machinery of the *T. cruzi* infection process, we decided to investigate the role of KIF5, a microtubule motor protein previously involved in directing VAMP7 vesicles to the cell periphery (Burgo et al., 2012; Fader et al., 2012), a phenomenon that was also observed in our system (Figure S4). For us to analyze the role of KIF5 in the transport of VAMP7 vesicles to the TcPV, CHO cells were co-transfected with GFP vector and either WT KIF5 or a negative mutant KIF5T93N, which is unable to bind to ATP and then infected with Try. Infection was quantified in each condition by confocal microscopy and compared to vector alone transfected cells. As shown in Figure 9b, the number of cells infected with parasites was significantly reduced in KIF5 mutant cells. In this experiment, we also detected endogenous VAMP7 by IF and observe the presence of VAMP7-positive vesicles around the TcPV in both vector and WT KIF5 cells (Figure 9a). As expected, recruitment of VAMP7 to the TcPV falls to approximately 30% in KIF5T93N cells (Figure 9a,c), demonstrating the importance of this kinesin in the VAMP7-positive vesicles arrival to the vacuole and *T. cruzi* infection.

3 | DISCUSSION

One of the most interesting characteristics of *T. cruzi* is its exceptional capacity to invade different types of mammalian cells. For us to achieve this, it exploits vesicular transport processes that lead to the formation of the TcPV, where the Try transitory resides until its release into the host cell cytoplasm. As described in Section 1, different membrane sources are engaged to the *T. cruzi* entry sites for the TcPV formation. In this regard, previously published works have demonstrated the participation of plasma membrane (Woolsey et al., 2003), endosomes (Wilkowsky et al., 2002), lysosomes (Tardieux et al., 1992; Andrade & Andrews, 2004), and autolysosomes (Romano et al.,

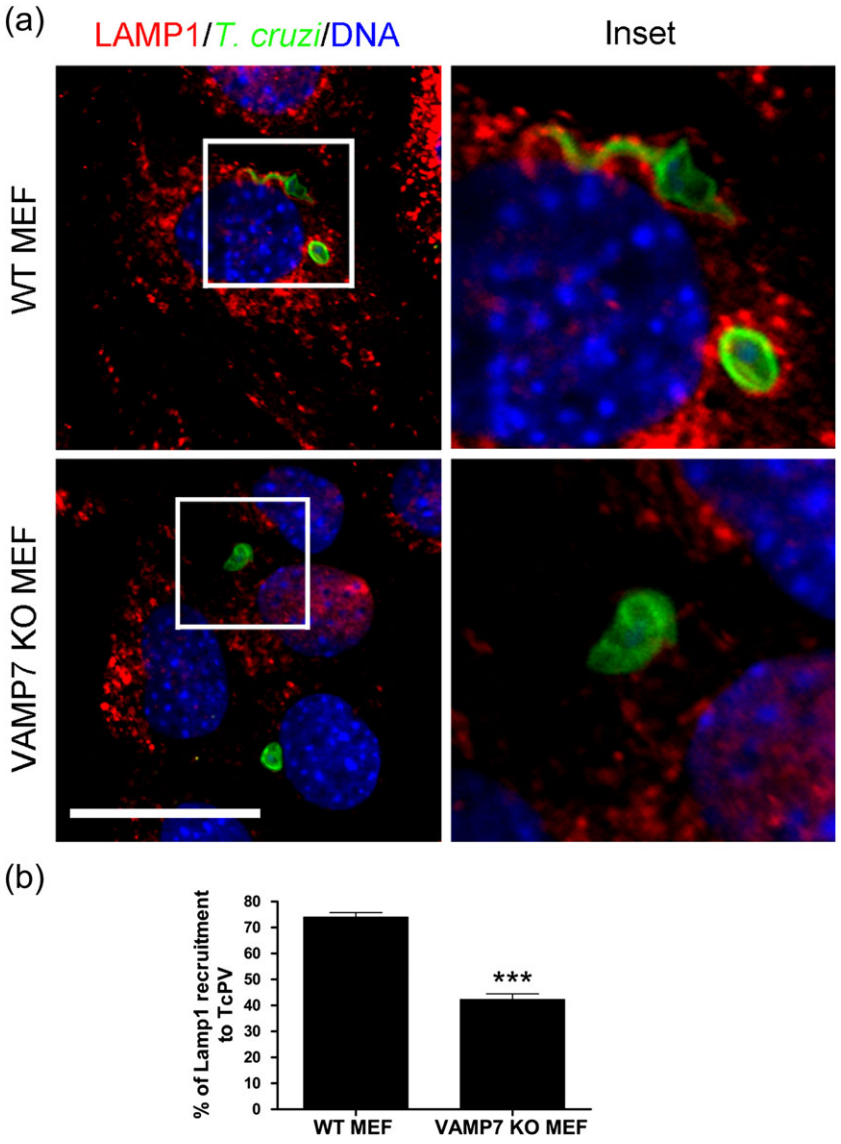

FIGURE 6 Effect of VAMP7 deficiency on LAMP1 recruitment to the *Trypanosoma cruzi* parasitophorous vacuoles. VAMP7 KO MEF cells and WT MEF cell were exposed to Try for 3 hr and then subjected to a double immunofluorescence to detect internalized parasites and LAMP1. (a) Confocal micrographs of a WT MEF cell infected with two parasites depicting LAMP1 labeling (upper panel) and an infected VAMP7 KO MEF exhibiting a parasites with a weak LAMP1 label (lower panel). Insets show higher magnification of framed regions. (b) Quantitative data indicate that a minor percentage of TcPVs recruit LAMP1 in VAMP7 KO MEF when compared with WT MEF cells. The data are represented as means ± SEM of three independent experiments. ***$p < .005$, Student's t test. Scale bar: 10 μm

2009), in this process. Among these, lysosomes and autolysosomes are particularly important because they confer the acidic environment required for vacuole maturation that enables the completion of the parasite intracellular life cycle (Ley et al., 1990; Andrade & Andrews, 2004; Romano et al., 2009). Based on these data, our aim was to identify which endosomal v-SNAREs are recruited and required for TcPV maturation. Our results unequivocally demonstrate an essential role of late endosomal/lysosomal VAMP7 in this process, whereas early endosomal VAMP3 recruitment appeared dispensable and VAMP8 was not recruited.

Firstly, our data show that inhibition of NSF activity by pretreatment of host cells with NEM or by expression of an NSF-dominant negative mutant results in a significant reduction of Try infection, indicating that functional SNAREs are required during the parasite entry process. Although low-infection values (~15%) are still observed under NSF inhibition conditions, it is possible that invagination of the plasma membrane, phenomena that do not require any fusion event, could explain this observation. In support of the last possibility, Woolsey et al. (2003) found that in cells treated with wortmannin or LY294002, which abrogates the lysosomal entry pathway, a remaining level of infection still occurred and these parasites were lodged in a plasma membrane-derived vacuole. In addition, the fact that overexpression of WT NSF increased the infection rate suggests that fusion events are highly stimulated during *T. cruzi* invasion and that the increased SNARE recycling, such as in NSF overexpressing cells, would benefit the process.

Because Try of CL Brener strain resides inside the vacuole for 6 hr previous to exit to the cytoplasm (Romano et al., 2009), we decided to infect cells for 3 hr to characterize the fusion machinery components at this intermediate time. At this time, we clearly showed that VAMP7 is the main v-SNARE recruited to the vacuole, followed by VAMP3 to a minor extent. It is thought that VAMP7 is involved in the fusion of lysosomes with late endosomes, other lysosomes, autophagosomes, and the plasma membrane (Galli et al., 1998; Ward, Pevsner, Scullion, Vaughn, & Kaplan, 2000; Pryor et al., 2004; Fader et al., 2009). On the other hand, VAMP3 regulates fusion of recycling endosomes and early endosomes with plasma membrane (McMahon et al., 1993; Miller et al., 2011). Our findings are in accordance with the major role of lysosomes (Woolsey et al., 2003; Andrade & Andrews, 2004; Woolsey & Burleigh, 2004) and autolysosomes (Romano et al., 2009) and a minimal but not negligible association with early or recycling endosomes during TcPV maturation (Wilkowsky et al., 2002; Woolsey et al.,

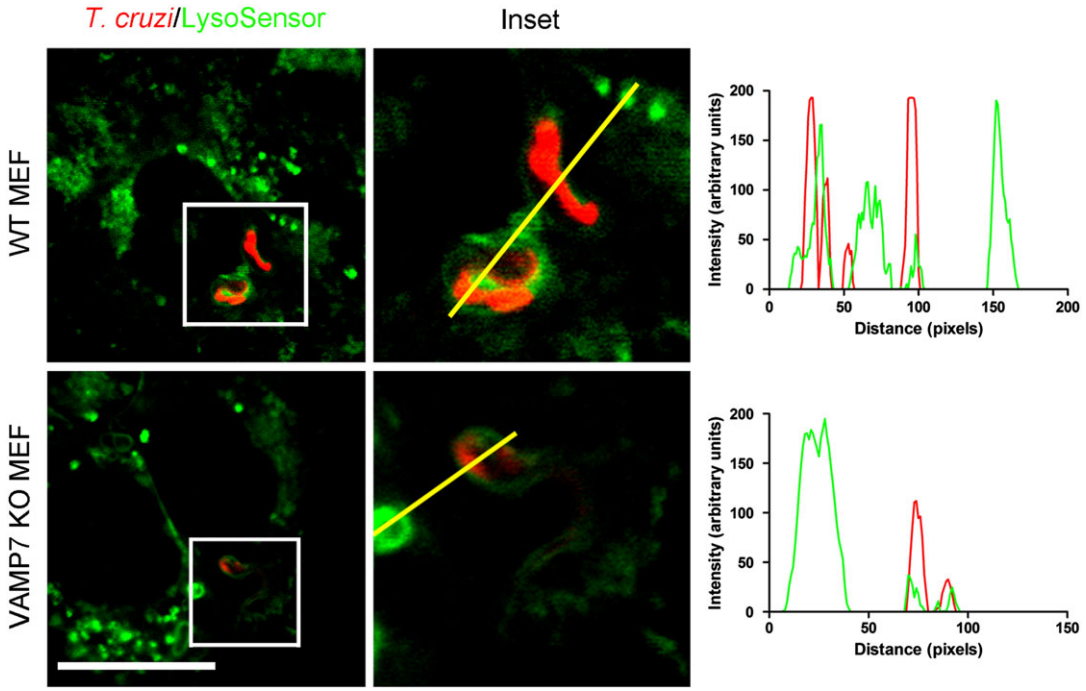

FIGURE 7 Effect of VAMP7 deficiency on *Trypanosoma cruzi* parasitophorous vacuoles acidification. VAMP7 KO MEF cells and WT MEF cells were exposed to LysoSensor and then infected with MytoTracker labeled Try for 2 hr. Live cells were visualized under confocal microscope. Micrographs show a WT MEF cell infected with two parasites (upper panel), one of them within a highly acidic TcPV and a VAMP7 KO MEF cell with a parasite inside a slightly acidic vesicle. Insets show higher magnification of framed regions. The yellow line in the merge panels indicates the pixels used for the RGB profile plots shown on the left. Scale bar: 10 μm

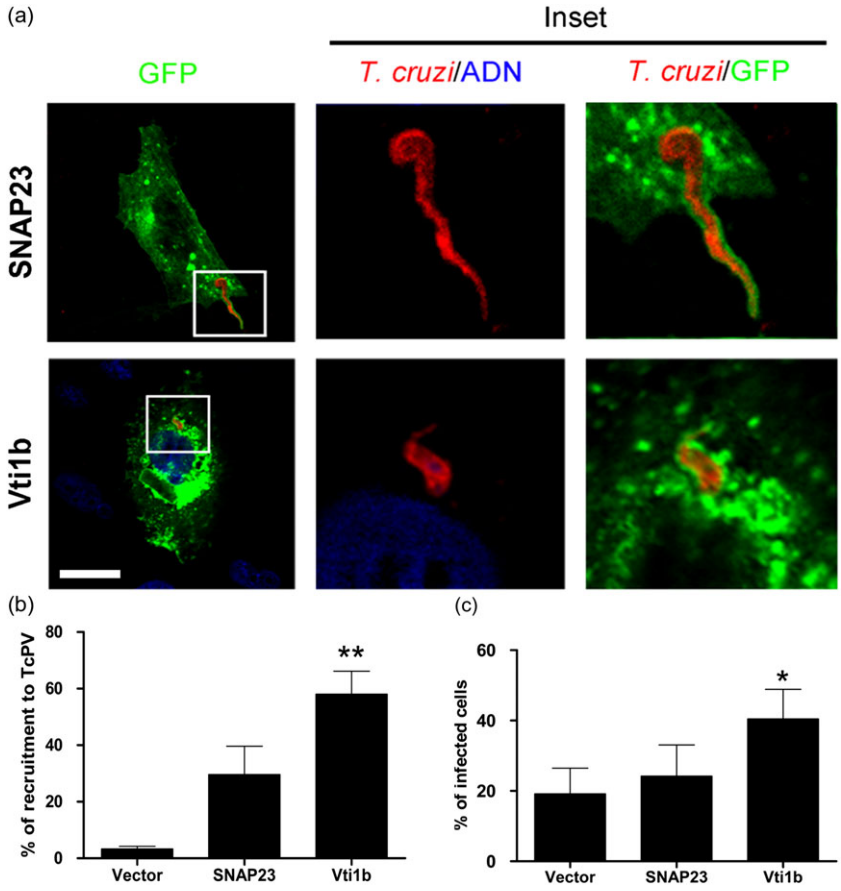

FIGURE 8 Recruitment of VAMP7 t-SNARE binding partners to *Trypanosoma cruzi* parasitophorous vacuoles. Chinese hamster ovary cells transiently expressing EGFP-Vti1b or EGFP-SNAP23 were infected with *T. cruzi* trypomastigotes for 3 hr. Cells were then fixed, subjected to indirect immunofluorescence to detect *T. cruzi*, and stained with Hoechst 33258 to visualize cell and parasite nuclei. (a) Confocal images show intracellular parasites associated with SNAP23, a plasma membrane t-SANRE (upper panel), and Vti1b, an endosomal t-SANRE (lower panel). Insets show higher magnification of framed regions. (b) Quantitative analysis shows high proportion of parasites associated with Vti1b and, to a lesser extent, with SNAP23. (c) The bar graph indicates that just Vti1b overexpression resulted in an increased infection rate. The data are represented as means ± SEM of three independent experiments. $^*p < .05$, Student's *t* test. Scale bar: 10 μm

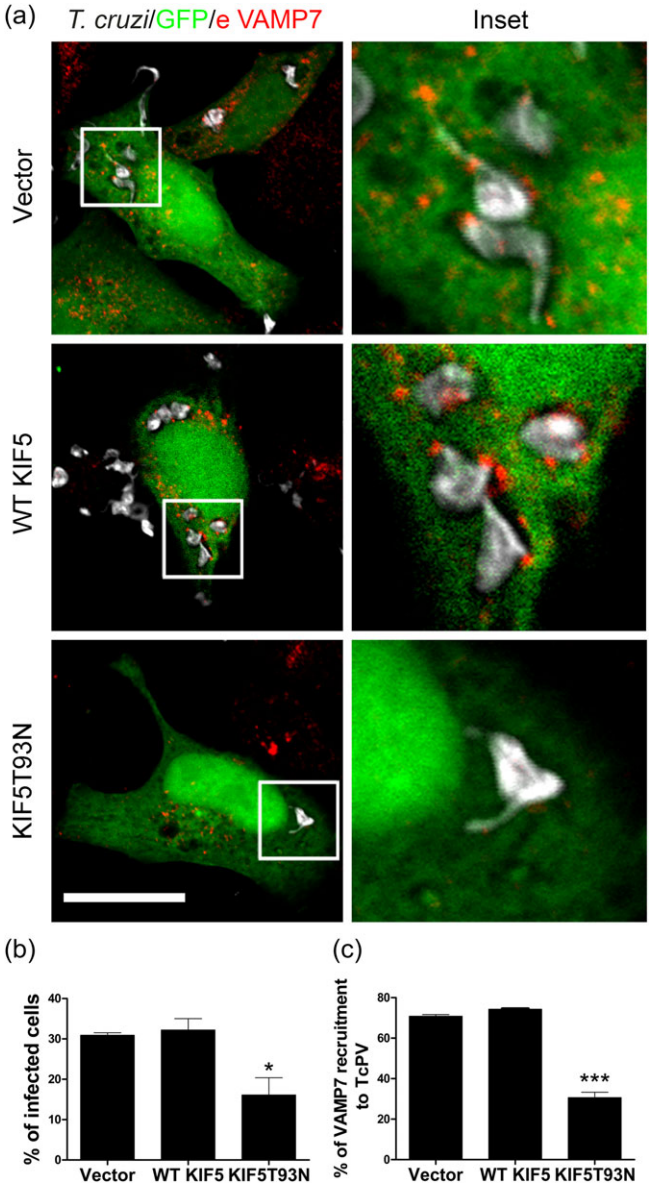

FIGURE 9 Effect of the overexpression of the Kinesin WT KIF5 and the dominant negative mutant KIF5 T93N on host cell infection. Chinese hamster ovary cells were co-transfected with EGFP vector and either pcDNA-KIF5 or pcDNA-KIF5 T93N. Parasites and endogenous VAMP7 were detected by double indirect immunofluorescence. (a) Confocal images showing a clear association between VAMP7 and TcPV in vector and WT KIF5-transfected cells (upper and middle panels, respectively) but not in KIF5 T93N (bottom panels). Insets show higher magnification of framed regions. (b) Quantification of the percentage of infected cells reveals that KIF5 T93N reduced susceptibility of host cell to infection. (c) Quantitative analysis shows a significant reduction in the host VAMP7 recruitment to the vacuole in KIF5 T93N-transfected cells, but WT KIF5 does not modified this parameter. The data are represented as means ± SEM of three independent experiments. *$p < .05$; ***$p < .005$, Student's t test. Scale bar: 10 μm

2003). However, VAMP8 was absent from the TcPV membrane, suggesting that homotypic fusions between late endosomes are not required in this process (Antonin, Holroyd, Tikkanen, Honing, & Jahn, 2000; Pryor et al., 2004).

Our kinetic studies showed a high percentage of VAMP3-labeled vacuoles at early times. This value remains high up to 1 hr p.i., abruptly decreasing after that. In contrast, the percentage of VAMP7-labeled vacuoles is low at the initial times of infection and gradually increases to reach a maximum value at 3 hr after infection. Beyond this time point, VAMP7-labeled vacuoles decreased, and no labeled parasites could be detected at 12-h p.i. Considering that VAMP3 is present in recycling or early endosomes, its major occurrence in the TcPV at the initial times is not surprising. In this regard, Wilkowsky et al. (2002) previously found the presence of early endosome markers (i.e., Rab5 and EEA1) in the newly formed TcPV before the interaction with lysosomes occurs. On the other hand, the timing of VAMP7 acquisition is in good agreement with the notion that interaction of lysosomes with TcPV results essential at later times for the intracellular retention of the parasite and the establishment of a productive infection. When the interaction with lysosomes is somehow inhibited, recently internalized parasites are able to exit host cell (Andrade & Andrews, 2004).

Because both VAMP3 and VAMP7 are specifically acquired by the TcPV membrane in a synchronized manner, we explored the requirement of these proteins for infection. Interestingly, our data show that proteolytic cleavage of either endogenous or overexpressed VAMP3 by TeNT did not alter the *T. cruzi* infection rate. Although VAMP3 recruitment was clearly observed during the *T. cruzi* vacuole formation, its action appears not to be critical for infection. In contrast, overexpression of the VAMP7 LD or VAMP7 depletion by siRNA treatment decreased the infection, indicating that VAMP7 fusion activity is required for this process. The significantly lower infection observed on VAMP7 KO MEF cells definitively demonstrates the essential role of VAMP7 in infection. The low-infection values still observed in the absence of VAMP7 could be explained by SNAREs functional redundancy (Wade et al., 2001).

Using VAMP7 KO MEF cells, we also observed a low-TcPV recruitment of the lysosomal marker LAMP1 and a weaker labeling with LysoSensor. In our kinetic studies, we also observed that Try gradually changed from the typical slender to a rounded form, suggesting that transition into Ama is initiated inside the vacuole. It is conceivable that the vacuolar acidic pH might be a key factor in this morphological transition because in vitro exposure of Try to an acidic culture medium induced their transformation into Ama (Kanbara, Uemura, Nakazawa, & Fukuma, 1990; Tomlinson, Vandekerckhove, Frevert, & Nussenzweig, 1995). Gradual acquisition of VAMP7-positive vesicles or acidic lysosomes by the TcPV reinforces this idea. Taking together, these results show that VAMP7 activity is required for the TcPV acquisition of lysosomal markers and acidity, essential requisites for infection. The high correlation between LAMP1 and VAMP7 recruitment kinetics supports this idea. Likewise, it is well established that the vacuolar acidic pH, conferred by lysosomes, triggers the parasite's mechanisms responsible for vacuole disruption and release of *T. cruzi* into the host cell cytoplasm (Ley et al., 1990). Here, we demonstrate that VAMP7 is a key protein in the necessary fusion of lysosomes to the *T. cruzi* vacuole.

Besides VAMP7, TcPV maturation is also regulated by Vti1b, an endosomal t-SNARE able to interact with VAMP7. We find that Vti1b is highly recruited to the TcPV at 3-hr p.i., and its overexpression increases cell infection. In contrast, SNAP23, a t-SNARE involved in

the fusion of VAMP7-positive vesicles with the plasma membrane, did not significantly modify the infection rate. These results support the idea that interaction of lysosomes with *T. cruzi* is not as immediate as proposed by the targeted lysosomes exocytosis model.

Our data further show that migration of VAMP7-positive vesicles to the TcPV depends on KIF5, a motor protein belonging to the superfamily of kinesins (Xie, 2010). KIF5 was previously implicated in microtubule-dependent VAMP7-positive vesicles trafficking to the periphery (Fader et al., 2012) likely via Varp recruitment of the kinesin (Burgo et al., 2012). By means of a transfection with a KIF5-negative mutant, we were able to inhibit VAMP7 recruitment to the TcPV and also the parasite infection rate, in good agreement with Rodríguez and coworkers (Xie, 2010) using microinjected antibody against kinesins.

An intriguing question concerning the role of the parasite on VAMP7 recruitment arises from this work: Is SNAREs recruitment a *T. cruzi*-driven process? Data coming from intracellular bacteria suggest that host VAMP7 could be actively modulated by secreted factors (Campoy et al., 2013; Delevoye et al., 2008). However, little is known about the *T. cruzi* factors that could mediate processes like these. Alternatively, *T. cruzi* could increase the activity rather than stimulate the recruitment of VAMP7. A recent report demonstrates that phosphorylation by c-Src kinase on longin domain positively regulate the VAMP7 fusogenic activity (Burgo et al., 2013). Interestingly, the c-Src pathway could be activated by integrins, integral membrane proteins that are recognized by Try (Caradonna & Burleigh, 2011), leading the possibility that *T. cruzi* could trigger a downstream cascade that finally would result in VAMP7 activation.

Although answering this question will require further research, in this work, we have clearly identified the molecular basis that takes place during the maturation of the TcPV. We showed that Try invasion process is characterized by the early and dispensable interaction with VAMP3-positive vesicles. Fusion of lysosomes with TcPV initiates afterwards, and it depends on the specific activity of VAMP7. Altogether, we demonstrated here a key role of VAMP7 in the TcPV maturation, a crucial process in the establishment of *T. cruzi* infection.

4 | EXPERIMENTAL PROCEDURES

4.1 | Reagents

Minimal essential medium (α-MEM) and Dulbecco-modified minimal essential medium (D-MEM) were obtained from Gibco Laboratories (Buenos Aires, Argentina). Fetal bovine serum (FBS) was purchased from Natocor S.A. (Córdoda, Argentina). Rabbit anti-*T. cruzi* polyclonal antibody was kindly provided by Dr. Catalina Alba (Instituto de Investigaciones en Microbiologia y Parasitologia Médica, Buenos Aires, Argentina). Endogenous VAMP7 was detected with a mouse anti-SYBL1 (mAb158.2, Abcam, ab36195, 58). Rabbit anti-LAMP1-Cy3 was from Sigma-Aldrich (Buenos Aires, Argentina). Vamp7 and scrambled siRNAs were obtained from Ambion (Texas, USA). The secondary Cy3 or Cy5 conjugated anti-mouse antibodies, Cy3 anti-rabbit antibody, LysoSens LysoSensor Green DND-189, and the DNA marker Hoechst 33342 were purchased from Life Technologies (Buenos Aires, Argentina). HRP-conjugated anti-mouse antibody was obtained from Jackson Immunoresearch Laboratories (Pennsylvania, USA). All other chemicals were from Sigma-Aldrich (Buenos Aires, Argentina).

4.2 | Plasmids

pEGFPC3 encoding GFP-VAMP8, GFP-VAMP3, GFP-VAMP7, and GFP-VAMP7 LD were previously characterized and are available at Addgene. pCMV5-TeNT was a generous gift from Dr. Heiner Niemann (Hannover Medical School, Hannover, Germany). The pEYFP-SNAP23 was gifted by Dr. Naohide Hirashima (Graduate School of Pharmaceutical Sciences, Nagoya, Japan). The pEGFP Vti1b was a gift of Dr. Alessandro Fraldi (Telethon Institute of Genetics and Medicine, Naples, Italy). The pCDNA KIF5, pCDNA KIF5T93N, was kindly provided by Dr. Alfredo Caceres (Instituto Mercedes y Martín Ferreyra, Córdoba, Argentina).

4.3 | Cell culture

Vero cells, a monkey epithelial cell line (obtained from ABAC, Asociación Banco Argentino de Células, Buenos Aires, Argentina) and HeLa human epithelial cells (ABAC) were grown in D-MEM supplemented with 10% FBS and antibiotics at 37 °C in an atmosphere of 95% air and 5% CO_2.

CHO cells (ABAC), were maintained in α-MEM supplemented with 10% FBS and antibiotics at 37 °C in an atmosphere of 95% air and 5% CO_2.

MEF WT and VAMP7 KO (obtained from C57BL/6 mice embryos, see below) were grown in D-MEM supplemented with 10% FBS and antibiotics at 37 °C in an atmosphere of 95% air and 5% CO_2.

4.4 | Culture and immortalization of mouse embryonic fibroblasts

Cells were harvested from WT and VAMP7 KO littermate E15 embryos resulting from crossing between C57BL/6-background (backcrossed >11) KO males and VAMP7 −/+ females (Molino et al., 2015). Only male embryos were used for cell culture as VAMP7 gene is located on the X chromosome. All animals were handled in strict accordance with good animal practice as defined by the national and/or local animal welfare bodies including local Ethics Committee (called CEEA40-Comité d'éthique Buffon at the Ministry of Higher Education and Research), and all mouse work was approved by the Veterinary Services of Paris (Authorization number: 75–1073). For immortalization, the "serial passages" method was used (Xu, 2005). MEFs passed their growth-crisis stage and were considered immortalized after at least 18 consecutive passages. Lack of VAMP7 expression in KO MEFs was assessed by Western blotting using mAb 158.2 and pAb TG50 as previously (Danglot et al., 2012).

4.5 | Propagation of *T. cruzi* trypomastigotes

CL Brener strains of *T. cruzi* were provided by Dr. Juan Jose Cazzulo (Inst. de Investigaciones Biotecnológicas. IIB-UNSAM, Bs. As., Argentina) and handled in a biosafety level II facility. Tissue cell Try was prepared as follows. Vero cells (5×10^5 cells/ml) were plated in

T25 flasks and maintained at 37 °C in D-MEM supplemented with 3% FBS and antibiotics (infection medium). Cells were infected with Try suspensions (5×10^6 cells/ml) for 3 days in infection medium at 37 °C in an atmosphere of 95% air and 5% CO_2. After 4 to 6 days, intracellular Try lysed the cells and reached the medium. Medium containing parasites was harvested and centrifuged at 600 × *g* for 15 min at room temperature. The supernatant was discarded, and the pellet, containing Try and Ama parasite forms, was covered with 1 ml of fresh infection medium and incubated for 3 hr at 37 °C to allow Try to swim up. Supernatant enriched in Try was harvested, and parasite concentration was determined using a Neubauer chamber and used for infection experiments.

4.6 | Immunofluorescence

Cells were fixed with 3% paraformaldehyde solution in PBS for 10 min at room temperature and quenched by incubating with 50 mM NH_4Cl in PBS. Afterwards, cells were permeabilized with 0.1% saponin in PBS containing 0.2% BSA and incubated with primary antibodies for 2 hr. Intracellular parasites were detected with a rabbit anti-*T. cruzi* polyclonal antibody (1:200), and endogenous VAMP7 was detected with the mouse anti-SYBL1 monoclonal antibody (dilution 1:100). Cy3-conjugated rabbit anti-LAMP1 was added at a 1:50 dilution when needed. Cells were subsequently incubated for 1 hr with Cy3 anti-rabbit (1:600), Cy3 anti-mouse (1:500), Alexa Fluor 488 anti-rabbit (1:400), or Cy5 anti-mouse (1:500) secondary antibodies as appropriate. Cells were also treated with Hoechst for DNA staining, mounted onto glass slides with Mowiol and analyzed with an Olympus Confocal Microscope FV1000-EVA (Olympus), with the FV10-ASW (version 01.07.00.16) software.

4.7 | Plasmids and siRNA cell transfections

CHO cells were plated on 13 mm round coverslips distributed in 24 well plates in α-MEM supplemented with 10% FBS and antibiotics. When the cultures reached 90% of confluence, they were transfected with plasmids (1 μg/μl) using the LipofectAMINE 2000 reagent (Thermo Fisher Scientific) according to the instructions of the manufacturer. Transfected cells were incubated for 24 hr in appropriate medium before being exposed to parasites.

For siRNA silencing experiments, HeLa cells were seeded on 13-mm round coverslips distributed in six well plates in D-MEM supplemented with 10% FBS and antibiotics. When cells grew to near 90% of confluence, they were co-transfected with EGFP vector and either siRNA against VAMP7 or scrambled siRNA using the LipofectAMINE 2000 reagent. After 5 hr, the transfection mix was replaced by fresh D-MEM with 10% FBS and incubated for an additional 48 hr. After that, round coverslips were transferred to 24 well plates, and cells were infected as explained further bellow. Remaining cells were used to quantify endogenous VAMP7 depletion by Western blot.

4.8 | Infection of cells with trypomastigotes

HeLa, CHO, VAMP7 KO MEF, or WT MEF cells attached on coverslips in 24 well plates were washed three times with PBS. Then a Try-enriched suspension was added at a multiplicity of infection of 20. Plates were subsequently centrifuged for 5 min at 4 °C to favor parasite–cell interaction. Infection was carried out for 3 hr at 37 °C unless indicated otherwise. Afterwards, extracellular parasites were removed by washing several times, and cells were subjected to IF.

4.9 | NEM treatment

CHO cells attached on coverslips in 24 well plates were washed twice briefly in PBS and were treated in PBS with 50 μM NEM or just PBS for 10 min on ice. The cells were then washed in PBS, incubated in culture medium for 30 min at 37 °C, and infected with Try.

4.10 | Live cell imaging

Two different experiments were run: In one case, we used CHO cells transfected with EGFP-VAMP7 plasmid and, in the other case, we used VAMP7 KO MEF and WT MEF treated with LysoSensor for 30 min. Cells were then infected with Try as described above, except that they were exposed to parasites for 2 hr. Previously, parasites were labeled during 30 min with red Mito Tracker dye (Molecular Probes) and washed three times with PBS before use. This marker labels the parasite mitochondrial network and allows in vivo visualization of parasites. After that, extracellular parasites were removed by washing, and the coverslip was placed in a temperature-controlled camera at 37 °C and analyzed with an Olympus FV100 Confocal Microscope. Movies were captured using the FV10 ASW 1.7 program and edited with Adobe® Photoshop® CS6.

ACKNOWLEDGMENTS

We are grateful to Alejandra Medero and Rodrigo Militello for technical assistance.

CONFLICT OF INTEREST

All authors have declared that no conflict of interests exists.

REFERENCES

Advani, R. J. (1999). VAMP-7 mediates vesicular transport from endosomes to lysosomes. *The Journal of Cell Biology*, *146*, 765–776.

Albertti, L. A. G., Macedo, A. M., Chiari, E., Andrews, N. W., & Andrade, L. O. (2010). Role of host lysosomal associated membrane protein (LAMP) in Trypanosoma cruzi invasion and intracellular development. *Microbes and Infection*, *12*, 784–789.

Andrade, L. O., & Andrews, N. W. (2004). Lysosomal fusion is essential for the retention of Trypanosoma cruzi inside host cells. *The Journal of Experimental Medicine*, *200*, 1135–1143.

Antonin, W., Holroyd, C., Tikkanen, R., Honing, S., & Jahn, R. (2000). The R-SNARE endobrevin/VAMP-8 mediates homotypic fusion of early endosomes and late endosomes. *Molecular Biology of the Cell*, *11*, 3289–3298.

Barrias, E. S., Reignault, L. C., Souza, W. D., & Carvalho, T. M. (2010). Dynasore, a dynamin inhibitor, inhibits Trypanosoma cruzi entry into peritoneal macrophages. *PloS One*, *5*, 1–11.

Barrias, E. S., Reignault, L. C., Souza, W. D., & Carvalho, T. M. U. (2012). Trypanosoma cruzi uses macropinocytosis as an additional entry pathway into mammalian host cell. *Microbes and Infection*, *14*, 1340–1351.

Bombardier, J. P., & Munson, M. (2015). Three steps forward, two steps back: Mechanistic insights into the assembly and disassembly of the SNARE complex. *Current Opinion in Chemical Biology*, *29*, 66–71.

Braun, W., Fraisier, V., Raposo, G., Hurbain, I., Sibarita, J. B., Chavrier, P., … Niedergang, F. (2004). TI-VAMP/VAMP7 is required for optimal phagocytosis of opsonised particles in macrophages. *EMBO J*, *23*, 4166–4176.

Breton, S., Nsumu, N. N., Galli, T., Sabolic, I., Smith, P. J. S., & Brown, D. (2000). Tetanus toxin-mediated cleavage of cellubrevin inhibits proton secretion in the male reproductive tract. *Am J Physiol Physiol*, *278*, 717–725.

Burgo, A., Casano, A.M., Kuster, A., Arold, S.T., Wang, G., Nola, S., … Galli, T. (2013) Increased activity of the vesicular soluble *N*-ethylmaleimide-sensitive factor attachment protein receptor TI-VAMP/VAMP7 by tyrosine phosphorylation in the longin domain. *The Journal of Biological Chemistry*, *288*, 11960–11972.

Burgo, A., Proux-Gillardeaux, V., Sotirakis, E., Bun, P., Casano, A., Verraes, A., … Galli, T. (2012). A molecular network for the transport of the TI-VAMP/VAMP7 vesicles from cell center to periphery. *Developmental Cell*, *23*, 166–180.

Caradonna, K. L., & Burleigh, B. A. (2011). Mechanisms of host cell invasion by trypanosoma cruzi. *Chagas Dis*, *33*.

Chaineau, M., Danglot, L., & Galli, T. (2009). Multiple roles of the vesicular-SNARE TI-VAMP in post-Golgi and endosomal trafficking. *FEBS Letters*, *583*, 3817–3826.

Caler, E. V., Chakrabarti, S., Fowler, K. T., Rao, S., & Andrews, N. W. (2001). The exocytosis-regulatory protein synaptotagmin VII mediates cell invasion by Trypanosoma cruzi. *The Journal of Experimental Medicine*, *193*, 1097–1104.

Campoy, E. M., Mansilla, M. E., & Colombo, M. I., (2013). Endocytic SNAREs are involved in optimal Coxiella burnetii vacuole development. *Cell Microbiol*, *15*, 922–941.

Cortez, C., Real, F., & Yoshida, N. (2015). Lysosome biogenesis/scattering increases host cell susceptibility to invasion by Trypanosoma cruzi metacyclic forms and resistance to tissue culture trypomastigotes. *Cellular Microbiology*.

Danglot, L., Zylbersztejn, K., Petkovic, M., Gauberti, M., Meziane, H., Combe, R., … Galli, T. (2012). Absence of TI-VAMP/Vamp7 leads to increased anxiety in mice. *The Journal of Neuroscience*, *32*, 1962–1968.

Daste, F., Galli, T., & Tareste, D. (2015). Structure and function of longin SNAREs. *Journal of Cell Science*, *128*, 4263–4272.

Delevoye, C., Nilges, M., Dehoux, P., Paumet, F., Perrinet, S., Dautry-Varsat, A., & Subtil, A., (2008). SNARE protein mimicry by an intracellular bacterium. *PLoS Pathog*, *4*, e1000022.

Fader, C. M., Aguilera, M. O., & Colombo, M. I. (2012). ATP is released from autophagic vesicles to the extracellular space in a VAMP7-dependent manner. *Autophagy*, *8*, 1741–1756.

Fader, C. M., Sánchez, D. G., Mestre, M. B., & Colombo, M. I. (2009). TI-VAMP/VAMP7 and VAMP3/cellubrevin: Two v-SNARE proteins involved in specific steps of the autophagy/multivesicular body pathways. *Biochim Biophys Acta (BBA)-Molecular Cell Res*, *1793*, 1901–1916.

Fernandes, M. C., Corrotte, M., Miguel, D. C., Tam, C., & Andrews, N. W. (2015). The exocyst is required for trypanosome invasion and the repair of mechanical plasma membrane wounds. *Journal of Cell Science*, *128*, 27–32.

Fernandes, M. C., Cortez, M., Flannery, A. R., Tam, C., Mortara, R. A., & Andrews, N. W. (2011). Trypanosoma cruzi subverts the sphingomyelinase-mediated plasma membrane repair pathway for cell invasion. *The Journal of Experimental Medicine*, *208*, 909–921.

Galli, T., Chilcote, T., Mundigl, O., Binz, T., Niemann, H., & Camilli, P. D. (1994). Tetanus toxin-mediated cleavage of cellubrevin impairs exocytosis of transferrin receptor-containing vesicles in CHO cells. *The Journal of Cell Biology*, *125*, 1015–1024.

Galli, T., Zahraoui, A., Vaidyanathan, V. V., Raposo, G., Tian, J. M., Karin, M., … Louvard, D. (1998). A novel tetanus neurotoxin-insensitive vesicle-associated membrane protein in SNARE complexes of the apical plasma membrane of epithelial cells. *Molecular Biology of the Cell*, *9*, 1437–1448.

Hotez, P. J., Dumonteil, E., Woc-Colburn, L., Serpa, J. A., Bezek, S., Edwards, M. S., … Bottazzi, M. E. (2012). Chagas disease: "The new HIV/AIDS of the Americas". *PLoS Neglected Tropical Diseases*, *6*, .e1498

Humeau, Y., Doussau, F., Grant, N. J., & Poulain, B. (2000). How botulinum and tetanus neurotoxins block neurotransmitter release. *Biochimie*, *82*, 427–446.

Kanbara, H., Uemura, H., Nakazawa, S., & Fukuma, T. (1990). Effect of low pH on transformation of Trypanosoma cruzi trypomastigote to amastigote. *Japanese J Parasitol*, *39*, 226–228.

Ley, V., Robbins, E. S., Nussenzweig, V., & Andrews, N. W. (1990). The exit of Trypanosoma cruzi from the phagosome is inhibited by raising the pH of acidic compartments. *The Journal of Experimental Medicine*, *171*, 401–413.

Martinez-Arca, S., Rudge, R., Vacca, M., Raposo, G., Camonis, J., Proux-Gillardeaux, V., … Filippini, F. (2003). A dual mechanism controlling the localization and function of exocytic v-SNAREs. *Proceedings of the National Academy of Sciences*, *100*, 9011–9016.

McMahon, H. T., Ushkaryov, Y. A., Edelmann, L., Link, E., Binz, T., Niemann, H., … Südhof, T. C. (1993). Cellubrevin is a ubiquitous tetanus-toxin substrate homologous to a putative synaptic vesicle fusion protein. *Nature*, *364*, 346–349.

Miller, S. E., Sahlender, D. A., Graham, S. C., Höning, S., Robinson, M. S., Peden, A. A., & Owen, D. J. (2011). The molecular basis for the endocytosis of small R-SNAREs by the clathrin adaptor CALM. *Cell*, *147*, 1118–1131.

Moeller, A., Zhao, C., Fried, M. G., Wilson-Kubalek, E. M., Carragher, B., & Whiteheart, S. W. (2012). Nucleotide-dependent conformational changes in the N-ethylmaleimide sensitive factor (NSF) and their potential role in SNARE complex disassembly. *Journal of Structural Biology*, *177*, 335–343.

Molino, D., Nola, S., Lam, S. M., Verraes, A., Proux-Gillardeaux, V., Boncompain, G., … Galli, T. (2015). Role of tetanus neurotoxin insensitive vesicle-associated membrane protein in membrane domains transport and homeostasis. *Cellular Logistics*, *5*, .e1025182

Nagiec, E. E., Bernstein, A., & Whiteheart, S. W. (1995). Each domain of the *N*-ethylmaleimide-sensitive fusion protein contributes to its transport activity. *The Journal of Biological Chemistry*, *270*, 29182–29188.

Proux-Gillardeaux, V., Raposo, G., Irinopoulou, T., & Galli, T. (2007). Expression of the longin domain of TI-VAMP impairs lysosomal secretion and epithelial cell migration. *Biology of the Cell*, *99*, 261–271.

Proux-Gillardeaux, V., Rudge, R., & Galli, T. (2005). The tetanus neurotoxin-sensitive and insensitive routes to and from the plasma membrane: Fast and slow pathways? *Traffic*, *6*, 366–373.

Pryor, P. R., Mullock, B. M., Bright, N. A., Lindsay, M. R., Gray, S. R., Richardson, S. C. W., … Luzio, J. P. (2004). Combinatorial SNARE complexes with VAMP7 or VAMP8 define different late endocytic fusion events. *EMBO Reports*, *5*, 590–595.

Rao, S. K., Huynh, C., Proux-Gillardeaux, V., Galli, T., & Andrews, N. W. (2004). Identification of SNAREs involved in synaptotagmin VII-regulated lysosomal exocytosis. *The Journal of Biological Chemistry*, *279*, 20471–20479.

Rassi, A., & Marin-Neto, J. A. (2010). Chagas disease. *Lancet (London, England)*, *375*, 1388–1402.

Romano, P. S., Arboit, M. A., Vázquez, C. L., & Colombo, M. I. (2009). The autophagic pathway is a key component in the lysosomal dependent entry of Trypanosoma cruzi into the host cell. *Autophagy*, *5*, 6–18.

Romano, P. S., Cueto, J. A., Casassa, A. F., Vanrell, M. C., Gottlieb, R. A., & Colombo, M. I. (2012). Molecular and cellular mechanisms involved in the Trypanosoma cruzi/host cell interplay. *IUBMB Life*, *64*, 387–396.

Schäfer, I. B., Hesketh, G. G., Bright, N. A., Gray, S. R., Pryor, P. R., Evans, P. R., … Owen, D. J. (2012). The binding of Varp to VAMP7 traps VAMP7 in a closed, fusogenically inactive conformation. *Nature Structural & Molecular Biology*, *19*, 1300–1309.

Tardieux, I., Webster, P., Ravesloot, J., Boron, W., Lunn, J. A., Heuser, J. E., & Andrews, N. W. (1992). Lysosome recruitment and fusion are early events required for trypanosome invasion of mammalian cells. *Cell*, *71*, 1117–1130.

Tomlinson, S., Vandekerckhove, F., Frevert, U., & Nussenzweig, V. (1995). The induction of Trypanosoma cruzi trypomastigote to amastigote transformation by low pH. *Parasitology*, *110*, 547–554.

Verderio, C., Cagnoli, C., Bergami, M., Francolini, M., Schenk, U., Colombo, A., … Danglot, L. (2012). TI-VAMP/VAMP7 is the SNARE of secretory lysosomes contributing to ATP secretion from astrocytes. *Biology of the Cell*, *104*, 213–228.

Wade, N., Bryant, N. J., Connolly, L. M., Simpson, R. J., Luzio, J. P., Piper, R. C., & James, D. E. (2001). Syntaxin 7 complexes with mouse Vps10p tail interactor 1b, syntaxin 6, vesicle-associated membrane protein (VAMP)8, and VAMP7 in b16 melanoma cells. *The Journal of Biological Chemistry*, *276*, 19820–19827.

Wang, C.-C., Shi, H., Guo, K., Ng, C. P., Li, J., Gan, B. Q., … Hong, W. (2007). VAMP8/endobrevin as a general vesicular SNARE for regulated exocytosis of the exocrine system. *Molecular Biology of the Cell*, *18*, 1056–1063.

Ward, D. M., Pevsner, J., Scullion, M. A., Vaughn, M., & Kaplan, J. (2000). Syntaxin 7 and VAMP-7 are soluble *N*-ethylmaleimide-sensitive factor attachment protein receptors required for late endosome-lysosome and homotypic lysosome fusion in alveolar macrophages. *Molecular Biology of the Cell*, *11*, 2327–2333.

Wilkowsky, S. E., Barbieri, M. A., Stahl, P. D., & Isola, E. L. D. (2002). Regulation of Trypanosoma cruzi invasion of nonphagocytic cells by the endocytically active GTPases dynamin, Rab5, and Rab7. *Biochemical and Biophysical Research Communications*, *291*, 516–521.

Woodman, P. G. (1997). The roles of NSF, SNAPs and SNAREs during membrane fusion. *Biochim Biophys Acta (BBA)-Molecular Cell Res*, *1357*, 155–172.

Woolsey, A. M., & Burleigh, B. A. (2004). Host cell actin polymerization is required for cellular retention of Trypanosoma cruzi and early association with endosomal/lysosomal compartments. *Cellular Microbiology*, *6*, 829–838.

Woolsey, A. M., Sunwoo, L., Petersen, C. A., Brachmann, S. M., Cantley, L. C., & Burleigh, B. A. (2003). Novel PI 3-kinase-dependent mechanisms of trypanosome invasion and vacuole maturation. *Journal of Cell Science*, *116*, 3611–3622.

Xie, P. (2010). Mechanism of processive movement of monomeric and dimeric kinesin molecules. *International Journal of Biological Sciences*, *6*, 665.

Xu, J. (2005). Preparation, culture, and immortalization of mouse embryonic fibroblasts. *Current Protocols in Molecular Biology*, *Chapter 28*, .Unit 28.1

Zhao, X., Kumar, P., Shah-Simpson, S., Caradonna, K. L., Galjart, N., Teygong, C., … Burleigh, B. A. (2013). Host microtubule plus-end binding protein CLASP1 influences sequential steps in the Trypanosoma cruzi infection process. *Cellular Microbiology*, *15*, 571–584.

Zhao, C., Smith, E. C., & Whiteheart, S. W. (2012). Requirements for the catalytic cycle of the *N*-ethylmaleimide-sensitive factor (NSF). *Biochimica et Biophysica Acta*, *1823*, 159–171.

SUPPORTING INFORMATION

Additional Supporting Information may be found online in the supporting information tab for this article.

How to cite this article: Cueto JA, Vanrell MC, Salassa BN, Nola S, Galli T, Colombo MI, Romano PS. Soluble *N*-ethylmaleimide-sensitive factor attachment protein receptors required during *Trypanosoma cruzi* parasitophorous vacuole development. *Cellular Microbiology*. 2016;e12713. doi: 10.1111/cmi.12713